Performance of a CO_2 Sorbent for Indoor Air Cleaning Applications: Effects of Environmental Conditions, Sorbent Aging, and Adsorption of Co-occurring Formaldehyde

Xiaochen Tang[1], Sébastien Houzé de l'Aulnoit[1], Mark T. Buelow[2], Jonathan Slack[1], Brett C. Singer[1], Hugo Destaillats[1,*]

1. Indoor Environment Group, Lawrence Berkeley National Laboratory, Berkeley CA, USA.

2. BASF Corporation, Iselin NJ, USA.

* Corresponding Author E-mail: HDestaillats@lbl.gov

RUNNING TITLE: *CO_2 sorbent for indoor air cleaning*

KEYWORDS: Carbon dioxide, Regenerative sorbent, HVAC, Formaldehyde.

Abstract

Indoor air cleaning systems that incorporate CO_2 sorbent materials enable HVAC load shifting and efficiency improvements. This study developed a bench-scale experimental system to evaluate the performance of a sorbent under controlled operation conditions. A thermostatic holder containing 3.15 g sorbent was connected to a manifold that delivered CO_2-enriched air at a known temperature and relative humidity (RH). The air stream was also enriched with 0.8 – 2.1 ppm formaldehyde. The CO_2 concentration was monitored in real time upstream and downstream of the sorbent, and integrated formaldehyde samples were collected at different times using DNPH-coated silica cartridges. Sorbent regeneration was carried out by circulating clean air in countercurrent. Almost 200 loading/regeneration cycles were performed in the span of 16 months, from which 104 were carried out at reference test conditions defined by loading with air at 25 °C, 38 % RH, and 1000 ppm CO_2 and regenerating with air at 80 °C, 3 % RH and 400 ppm. The working capacity decreased slightly from 43–44 mg CO_2 per g sorbent to 39–40 mg per g over the 17 months. The capacity increased with lower loading temperature (in the range 15–35 °C) and higher regeneration temperature, between 40 and 80 °C. The CO_2 capacity was not sensitive to the moisture content in the range 6 – 9 g m^{-3}, and decreased slightly when dry air was used. Loading isothermal breakthrough curves were fitted to three simple adsorption models, verifying that pseudo-first order kinetics appropriately describes the adsorption process. The model predicted equilibrium capacities decreased with increasing temperature from 15 to 35 °C, while adsorption rate constants slightly increased. The formaldehyde adsorption efficiency was 80-99% in different cycles, corresponding to an average capacity of 86 ± 36 µg g^{-1}. Formaldehyde was not quantitatively released during regeneration, but its accumulation on the sorbent did not affect CO_2 adsorption.

Practical Implications

Air cleaning technologies that remove CO_2 and other indoor-generated pollutants can be used to increase the amount of air that is recirculated in buildings, reducing the fraction of outdoor air used in ventilation to enable peak load reductions and energy savings. In addition, the tested CO_2 sorbent was shown to be effective in capturing formaldehyde, a ubiquitous indoor pollutant that is often difficult to remove with most VOC air cleaning technologies.

1 Introduction

Commercial buildings account for 18% of U.S. energy consumption, releasing approximately 1000 Tg carbon dioxide (CO_2) y^{-1} to the atmosphere, which amount to 18% of the US, and 3% of the global anthropogenic emission rate [1, 2]. Improving building efficiency thus can help carbon abatement on a national and global scale. For commercial buildings in the US, an estimated 9.5% of end-use energy is required for ventilation, heating and cooling [3]. Furthermore, heating, ventilation and air conditioning (HVAC) systems are particularly energy intensive during peak electricity demand, which is costly and adds strain to the grid. Reducing the rate of outdoor air supply is an effective measure to decrease both peak loads and energy consumption in a building. However indoor-originated pollutants (primarily CO_2, other bioeffluents, and volatile organic compounds) can accumulate with lower air change rate and negatively impact occupant performance, indoor air quality perceptions, and building-related symptoms [4-6].

CO_2 has been used for a long time as a surrogate for human bioeffluents in buildings [7]. The ANSI/ASHRAE Standard 62.1-2016 "Ventilation for acceptable indoor air quality" (Appendix D) stipulates that if indoor CO_2 concentration do not exceed 700 ppm above outdoor levels, a substantial majority of visitors entering a space will be satisfied with respect to human bioeffluents" [8]. High occupant densities in inadequately ventilated spaces can generate indoor CO_2 levels that largely exceed this limit. For example, Seppänen et al. reported indoor CO_2 levels as high as 3700 ppm in offices and 2800 ppm in schools [9]. Recent studies have shown that moderate and elevated indoor CO_2 levels can have adverse impacts on cognitive performance, comprising functions such as developing strategies, taking initiatives, searching and using information, among others [10-13]. These initial studies should be supported by additional research to provide a consistent quantitative picture on the potential impact, to investigate effects of CO_2 levels on children and sensitive populations (e.g., people with health problems and the elderly), and to investigate long-term effects of continuous and periodical exposures to CO_2 [14].

Active CO_2 removal in commercial buildings has the potential to provide better indoor air quality, reduce peak loads and save energy by reducing the need for outdoor air ventilation when outdoor air is particularly polluted and/or requiring substantial tempering. Such CO_2-removing technologies implemented in HVAC systems may also remove other indoor pollutants of

concern. Among technologies to capture CO_2 from air, amine-functionalized materials are promising because of their high selectivity at low concentrations [15], tolerance to moisture due to the chemical rather than physical nature of the sorbent–adsorbate interaction [16], and long-term stability [15]. Amines can be coated onto different substrates, including zeolites [17, 18], silica [15, 19-22], diatomaceous earth [23], and activated carbon [24], yielding capacities that are in most cases in the range 10 – 100 mg CO_2 per g of sorbent. Two main mechanisms are postulated for the chemical interaction of CO_2 with surface-functional primary or secondary amine groups on the solid sorbent material [19, 25-28]. Under dry conditions (RH ~0%), carbamates are formed according to Eq. (1), as follows:

$$2(RR'NH) + CO_2 \leftrightarrow RR'NCO_2^- + RR'NH_2^+ \quad (1)$$

where R and R' may be organic substituents or H atoms. In the presence of moisture, bicarbonates are formed according to Eq. (2):

$$RR'NH + CO_2 + H_2O \leftrightarrow RR'NH_2^+ + HCO_3^- \quad (2)$$

Other contaminants are often present in the gas stream containing CO_2, and can interact with the amine-impregnated adsorbents. For example, studies described the adsorption of CO_2 in the flue gas of a natural gas fired boiler, in the presence of N_2, O_2, CO and NO_x [27, 29]. In building applications, volatile organic compounds (VOCs) are other contaminants are being treated along with CO_2. Formaldehyde is a particularly relevant VOC as it is ubiquitous in buildings and very often at levels that exceed the California Office of Environmental Health Hazard Assessment (OEHHA) chronic reference exposure level of 9 μg m^{-3}. Formaldehyde is emitted by building materials, insulation, consumer products, and combustion. Exposure to formaldehyde at elevated concentrations causes irritation of the respiratory tract membrane and eyes [30, 31]. Due to its high volatility, most sorbent-based technologies are not particularly effective at removing formaldehyde; for that reason, thermal regenerative systems are particularly promising for the abatement of this compound [32, 33]. In the case of amine-based sorbents, formaldehyde and other carbonyls can be trapped by chemisorption through the formation of imines (Schiff base) [21, 23, 34-36]. Similarly, carboxylic acids were shown to chemisorb through acid-base interactions [37].

CO_2 adsorption kinetic data are important for the design of a CO_2 removal system, and simulation of its operation as a component of a building's HVAC system. Adsorption capacity

and rate determine the amount of sorbent required for the system, thus influencing device size and capital cost [20, 38]. A wide variety of kinetic models of different complexities have been developed to quantitatively describe the adsorption processes, and to identify the adsorption mechanism. Due to the complexities associated with the exact description of kinetic parameters, a common approach involves fitting the experimental results to conventional kinetic models, and selecting the model with the best fit [15, 20]. Accordingly, three of the most common theoretical kinetic models previously applied to describe the adsorbent−adsorbate interactions and adsorption rate behaviour were used in this study: the pseudo-first-order, pseudo-second-order, and Avrami models [24].

This study evaluated the performance of a sorbent material that removes CO_2 and formaldehyde from indoor air and has the potential to treat these contaminants for ventilation management in commercial buildings. With the objective of advancing the use of sorbent-based air cleaning in commercial buildings, we developed test methods and metrics, and then measured systematically their performance under a range of conditions that may be encountered when deployed in a building-scale system. This information is needed to incorporate the tested sorbents into air quality management systems. The results of this material characterization study can be directly integrated to the development and application of simulation tools that can serve as predictive methodologies to identify optimal operation conditions in specific buildings and climates.

2 Methods

2.1 Sorbent material

The tested material was provided by BASF Corporation (Iselin, NJ). It is a granulated silica coated with a polyamine, having granule size between 0.5 and 1.0 mm, prepared according to methods described in a patent application [39]. This material can be readily scaled-up for application in buildings. In this study, 3.15 g (4.5 cm^3) fresh sorbent was placed in a holder, in which the material remained during the testing process, including periods between experiments, when no air flow circulated through the sorbent.

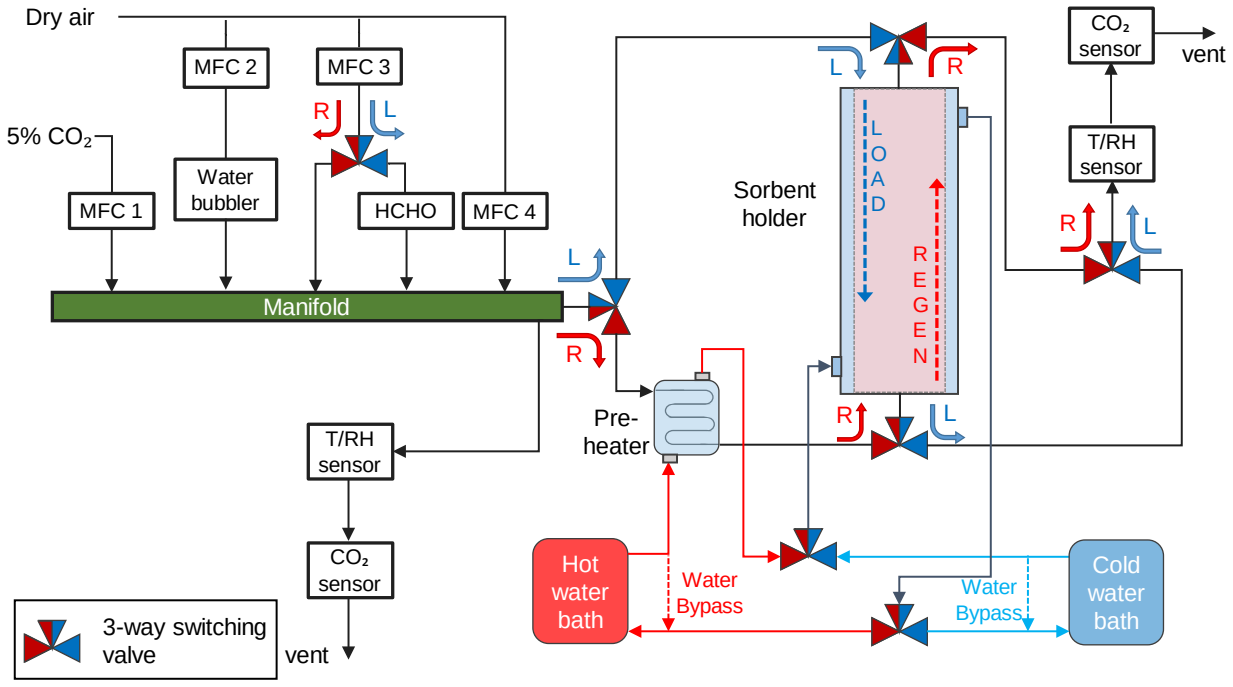

Figure 1. Schematic of the experimental setup. The 3-way switching valves enable the flow to follow either loading (L) or regeneration (R) conditions in each period, respectively. Air flow was adjusted using mass flow controllers (MFC).

2.2 Experimental apparatus

A fully-automated experimental apparatus was designed and built at Lawrence Berkeley National Laboratory (LBNL) to evaluate the performance of the sorbent material under various conditions, as shown in Figure 1. A cylindrical sorbent holder was made of stainless steel, 2.5 cm in internal diameter and 10 cm long, wrapped by a built-in water jacket that allowed accurate temperature control with circulating water. Two dense steel wire mesh plates were fixed at the top and bottom of the holder, confining the sorbent material inside regardless of the air flow direction. A manifold was used to prepare a gas mixture upstream of the holder. It combined four streams of gases: 1) CO_2 (5% balanced with air, Praxair), 2) formaldehyde-enriched air during loading, or pure dry air during regeneration, 3) humidified air, and 4) balance dry air. The flow rate of each stream was controlled individually by mass flow controllers (Alicat Scientific, Inc).

The dry, CO_2-free air was generated with a pure gas generator (Parker Balston Model 75-45NA, Parker Hannifin Corporation). Humidified air was generated by passing dry air through a water bubbler prior to entering the chamber. The formaldehyde source consisted on a beaker containing solid paraformaldehyde (polyoxymethylene 95%, Millipore Sigma) housed inside a glass flow cell at room temperature. Introduction of dry air led to a formaldehyde-enriched steady-state air flow. An analytical standard of the formaldehyde derivative dinitrophenyl hydrazone (Millipore Sigma) was used to identify and quantify formaldehyde. Carbonyl-free acetonitrile (⩾99.9%, Honeywell) was used for cartridge extraction and as HPLC mobile phase.

The total flow rate exiting the manifold was 1.3 L min^{-1}, from which 0.3 L min^{-1} was drawn by the upstream CO_2 analyzer, and the remaining 1.0 L min^{-1} entered the sorbent holder. Relative humidity (RH) was controlled by adjusting the relative ratios of dry and humidified air, keeping the total flow rate of 1 L min^{-1}. Two CO_2 gas analyzers (SBA-5, PP Systems) were used to measure CO_2 concentration continuously, upstream and downstream of the sorbent. Once before and during the study, four-point calibrations were conducted to ensure linearity and accuracy of CO_2 measurements. In line with the CO_2 analyzers, RH of the air entering and exiting the chamber was monitored with an in-line digital sensor (HIH6100 series, Honeywell) and recorded in real time. RH was measured at ambient temperature in all cases (20 °C), from which the moisture content (absolute humidity) was calculated, and used to predict the RH at the working temperature inside the sorbent holder during loading and regeneration.

Two digitally-controlled thermostatic water circulators were used to maintain a constant sorbent temperature during the loading and regeneration phases. One of them was used to keep the desired (moderate) temperature in the sorbent holder during the loading phase. During regeneration, hot water from the other thermostat flowed through an air pre-heating apparatus before entering the sorbent holder's water jacket. The pre-heater was a sealed 1 L copper vessel housing a 100 cm copper tube serpentine carrying the air flow from the manifold to the sorbent holder. A bypass loop connected to a six-port valve enabled the continuous circulation of water from the thermostat that was not in use during each phase of the experiment. The holder, pre-heater, valve and tubing were insulated with a 2.5 cm layer of polyethylene foam to minimize heat losses.

The holder temperature was monitored with a K-type thermocouple in direct contact with the metallic outside wall, underneath the insulation. Working temperature was also monitored with another thermocouple placed directly on top of the upper mesh plate without direct contact with metal parts, thus measuring the air flow temperature entering the chamber during loading, and exiting during regeneration. A data logger thermometer (HH309A, Omega) recorded the holder and air temperatures at a rate of 0.5 Hz.

2.3 System operation

The system was operated cyclically by switching on a continuous basis between loading and regeneration mode. The loading CO_2 concentration was 1000 – 1600 ppm, representing commonly found levels in buildings with high-occupancy, and the regeneration concentration was 400 ppm to simulate the use of clean outdoor air. Formaldehyde was only introduced during loading, at concentrations between 0.8 and 2.1 ppm. Those concentrations are between one and two orders of magnitude higher than typical levels found in US commercial buildings [40, 41]. The sorbent was challenged with a higher than typical formaldehyde concentrations to perform an accelerated capacity test. This is a common approach in early-stage bench-scale evaluation, which assumes that the uptake of the contaminant is not a function of the concentration. During loading, the air temperature was in the range 15 – 35 °C, and the corresponding relative humidity at the working temperature was between ~0 (dry air) and 68 %. Regeneration temperatures were between 40 and 80°C. The relative humidity during regeneration was between ~0 (dry air) and 17 %. Reference test conditions were defined by a loading temperature of 25 °C, loading RH of 38%, regeneration temperature of 80 °C, and regeneration RH of 3%. All test conditions are reported in Table 1.

Air flowed through the sorbent from top to bottom during the loading phase and the direction was reversed during regeneration. Switching between loading and regeneration mode was enabled by automatically actuated valves, controlled by lab-built electronic control boards that were reading the downstream CO_2 concentration. The end of the loading phase was set when the CO_2 concentration in the effluent air reached 900 ppm. For the end of the regeneration phase, a CO_2 effluent concentration of 410 ppm was chosen. These target levels, which were respectively lower and higher than the upstream CO_2 levels, were selected for rapid operation, avoiding lengthy asymptotic processes when the material was quasi saturated or almost fully regenerated.

When signals were received from the control boards, the automatic switching valves 1) adjusted CO_2 concentration, 2) reversed air flow direction, 3) determining whether formaldehyde was introduced or bypassed, and 4) switched the thermostat connected to the sorbent holder.

2.4 Evaluation of CO_2 adsorption/desorption capacity

The metrics used to evaluate the sorbent performance were the working adsorption and desorption capacities, reported in mass of CO_2 per mass of sorbent. The time for the sorbent to reach equilibrium is impractically long to use equilibrium capacity as a performance measure. Rather, working capacities that are defined for shorter adsorption times are more useful for evaluation. In this study, the working adsorption capacity was determined for downstream CO_2 concentrations reaching 900 ppm, which is 90% of the upstream levels for practically all tested conditions (except for tests at upstream CO_2 = 1600 ppm). For that reason, the working capacity was always lower than the equilibrium capacity of the sorbent. The working regeneration capacity was determined for downstream CO_2 concentrations approaching 410 ppm, in all cases.

The mass of adsorbed and desorbed CO_2 was determined by integrating the time-resolved CO_2 concentration of the airstream upstream and downstream of the sorbent during loading and regeneration phases, and multiplying by the air flow rate (Eqs. 3 and 4). The CO_2 analyzers recorded CO_2 concentrations every 1.6 s, which were averaged every minute. The difference between the beginning and end of the loading and regeneration cycles was computed as follows:

$$\Delta m_{CO_{2,ad}} = Q \times \sum\left([CO_2]_{up} - [CO_2]_{dn}\right) \quad (3)$$

$$\Delta m_{CO_{2,de}} = Q \times \sum\left([CO_2]_{dn} - [CO_2]_{up}\right) \quad (4)$$

where $\Delta m_{CO_{2,ad}}$ and $\Delta m_{CO_{2,de}}$ are the mass of CO_2 being adsorbed and desorbed in the loading and regeneration phase, respectively (expressed in mg). Q is the air flow rate (1 L min^{-1}) and $[CO_2]_{up}$ and $[CO_2]_{dn}$ are the upstream and downstream CO_2 concentration, respectively (expressed in µg m^{-3}). The adsorption and desorption working capacity ($C_{CO_{2,ad}}$ and $C_{CO_{2,de}}$, expressed in mg CO_2 per gram of sorbent) were calculated by dividing the mass of captured or released CO_2 by the mass of sorbent in the chamber following Eqs. (5) and (6):

$$C_{CO_{2,ad}} = \frac{\Delta m_{CO_{2,ad}}}{m_{sorbent}} \quad (5)$$

$$C_{CO_{2,de}} = \frac{\Delta m_{CO_{2,de}}}{m_{sorbent}} \quad (6)$$

The working capacity for each condition was calculated as the average of values determined in a number of loading and regeneration cycles, and the experimental error is one standard deviation of those determinations.

The real-time CO_2 breakthrough curves illustrated in Figure 2 describe the adsorption and desorption behavior of the sorbent. During the loading phase, the downstream CO_2 concentration increased slowly, approaching asymptotically the challenge CO_2 concentration. In the regeneration phase, as the sorbent temperature increased sharply, a CO_2 spike occurred initially in a very short period, with a peak concentration up to almost 3000 ppm, followed by gradually decreasing concentrations. The CO_2 capacity was a function of the arbitrarily selected endpoints of the loading and regeneration breakthrough curves, and it increased as the endpoints approached the challenge concentrations. During initial method development, three different loading endpoints were evaluated at 700, 800 and 900 ppm (Table S1, Supporting Information). The endpoints of 900 ppm (loading) and 410 ppm (regeneration) were chosen to combine high capacity with relatively short cycle duration.

2.5 Evaluation of formaldehyde adsorption/desorption capacity

All formaldehyde (HCHO) measurements were made under the previously defined reference testing conditions. Formaldehyde was collected simultaneously upstream and downstream of the chamber using a peristaltic pump connected to a 2,4-dinitrophenylhydrazine (DNPH)-impregnated silica gel cartridges (Waters Corp., United States). Sample flow through each DNPH cartridge was ~80 mL min^{-1}. The duration of each sample coincided with that of individual loading or regeneration periods, between 2 and 4 hours. Formaldehyde samples were collected on a sub-set of loading/regeneration (L/R) cycles for each test. The cartridges were extracted with 2 mL of carbonyl-free acetonitrile and analyzed by High Performance Liquid Chromatography (HPLC) with UV detection (Agilent 1200), following the EPA TO-11 method.[42]. A calibration curve was generated for quantification of formaldehyde using an authentic standard of the formaldehyde hydrazone.

Similar to the analysis described above for CO_2, adsorption and desorption capacity of formaldehyde ($C_{HCHO_{ad}}$ and $C_{HCHO_{de}}$, expressed in mg formaldehyde per g sorbent) were evaluated based on the amounts retained and released during the loading and regeneration period, respectively. The amounts measured in each cycle varied with the changes in loading concentration of formaldehyde due to fluctuation in its generation system, leading to upstream concentrations in the range 0.8 ppm to 2.1 ppm, with an average value of 1.5 ± 0.6 ppb. The adsorption and desorption efficiency (f_{ad} and f_{de}, expressed in %) were introduced as additional metrics for the quantification of formaldehyde capture performance, calculated using Eqs. (7) and (8). The parameter $\Delta m_{HCHO_{load}}$ is the total mass of formaldehyde in the challenge gas stream during the loading period, a fraction of which, $\Delta m_{HCHO_{ad}}$, is the amount retained by the sorbent. The desorption efficiency, f_{de}, is defined as the relative fraction of released formaldehyde in the effluent ($\Delta m_{HCHO_{de}}$) compared with the amount retained in the preceding loading cycle ($\Delta m_{HCHO_{ad}}$).

$$f_{ad} = \frac{\Delta m_{HCHO_{ad}}}{\Delta m_{HCHO_{load}}} \times 100 \quad (7)$$

$$f_{de} = \frac{\Delta m_{HCHO_{de}}}{\Delta m_{HCHO_{ad}}} \times 100 \quad (8)$$

Since $\Delta m_{HCHOload}$ and Δm_{HCHOad} were determined by sampling formaldehyde simultaneously upstream and downstream of the sorbent, the determined adsorption efficiency, f_{ad}, is not sensitive to fluctuations in upstream formaldehyde concentrations. Similarly, the two quantities used in the computation of the desorption efficiency, f_{de}, while not measured simultaneously, are strongly correlated because they correspond to the same L/R cycle.

2.6 Evaluation of the effect of residence time on CO_2 adsorption capacity

Four tests were carried out using a separate experimental setup that allowed for circulation of air through the sorbent at higher flows, to evaluate the effect of residence time (R_t), or face velocity. In these tests, 12.6 g of the sorbent were placed in a cylindrical bed, with a depth of 25 mm. Adsorption isothermal breakthrough curves were recorded by challenging the sorbent with approximately 1000 ppm CO_2 at 30 °C, at four different air flows: 56, 28, 14 and 5.6 L min^{-1}. These flows corresponded to residence times of 25, 50, 100 and 250 ms, and to face velocities of

1, 0.5, 0.25 and 0.1 m s^{-1}, respectively. Loading was carried out using dry air (0% RH). After each loading breakthrough curve was recorded, CO_2 was desorbed with air containing 400 ppm CO_2 at 65 °C with a flow of 11 L min^{-1}. A 1% V/V water was added to the regeneration air, equivalent to a moisture content of 7.4 g m^{-3}, corresponding to a relative humidity RH = 4% at the regeneration temperature. The same sorbent sample was used consecutively for the four determinations. A breakthrough curve was determined only during the loading phase, but not during regeneration, for each condition. The working capacity was determined in each case using Eqs. (3) and (5). The experimental error assigned to single determinations was estimated from the uncertainty in the upstream CO_2 concentration measurements, $[CO_2]_{up}$.

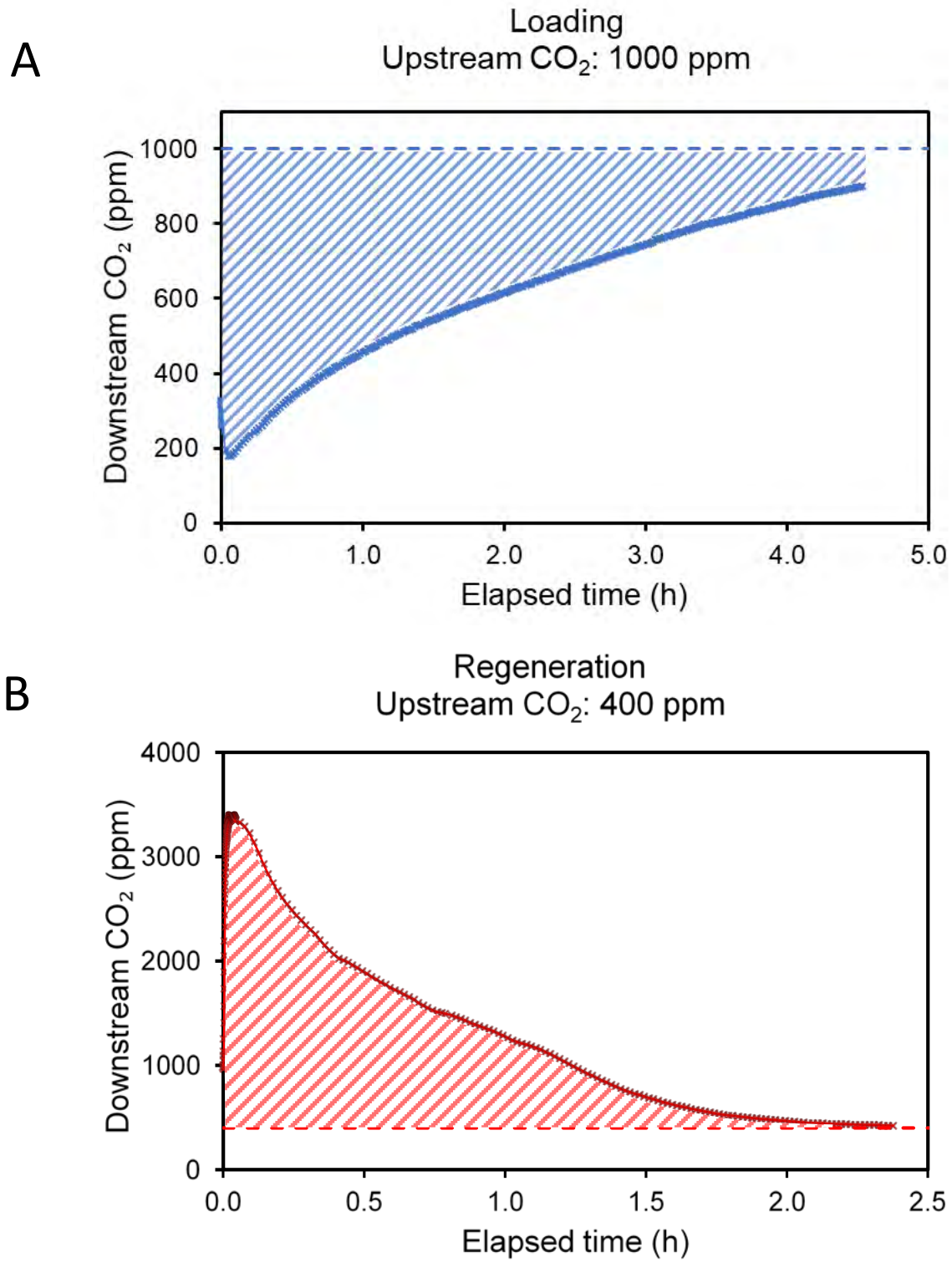

Figure 2. Isothermal breakthrough curves corresponding to (A) Loading at 25 °C, and (B) Regeneration at 80 °C. The shaded areas between the curve and the challenge CO_2 concentration are proportional to the mass of CO_2 adsorbed during loading, and desorbed during regeneration.

3. Results and Discussion

The CO_2 loading and regeneration working capacities determined under different experimental conditions are listed in Table 1. Nearly 200 loading/regeneration cycles were performed using the same sorbent material in different experiments carried out over a 17-month period (June 2017 to October 2018). Tests carried out in reference conditions allowed for an evaluation of the sorbent's performance under typical building operation conditions. Those tests were repeated at different times, allowing for an evaluation of changes in performance as the material aged (section 3.1). Other tests evaluated the impact of higher CO_2 upstream concentrations (section 3.2), and the effects of loading temperature, regeneration temperature, and loading relative humidity (section 3.3). The results were rationalized using simple partitioning models (section 3.4). Finally, the material's retention efficiency for formaldehyde was quantified (section 3.5).

3.1 CO_2 adsorption and desorption under reference test conditions

After initial evaluation of several conditions (June-July 2017), the reference testing conditions were established as 25 °C, 38 ± 5% RH and 1 atm pressure for adsorption (loading), and 80 °C, 3% RH and the same pressure for desorption (regeneration). For both loading and regeneration, the relative humidity measured at room temperature (20 °C) far from the sorbent holder was 50 ± 5%. The challenge CO_2 concentration was 1000 ppm and 400 ppm for loading and regeneration, respectively.

Table 1. Working capacity determined under various experimental conditions (cutoff target during loading: 900 ppm)

Test	Date	# of L/R cycles	Challenge CO_2 conc. (ppm)	Residence time (ms)	Loading				Regeneration			
					T (°C)	RH (%)	Moisture content (g m^{-3})	Working capacity (mg CO_2 per g sorbent)	T (°C)	RH (%)	Moisture content (g m^{-3})	Working capacity (mg CO_2 per g sorbent)
Reference test conditions	9/2017	32	1000	270	25	38	8.7	43 ± 2	80	3	8.7	44 ± 2
	10/2017	29	1000	270	25	38	8.7	45 ± 2	80	3	8.7	45 ± 3
	4/2018	36	1000	270	25	38	8.7	40 ± 1	80	3	8.7	43 ± 2
	8/2018	4	1000	270	25	38	8.7	40 ± 1	80	3	8.7	41 ± 1
	10/2018	3	1000	270	25	38	8.7	39 ± 1	80	3	8.7	40 ± 1
Loading CO_2 level	6/2017	5	1600	270	25	38	8.7	30 ± 1	80	3	8.7	34 ± 1
Loading temperature	7/2017	7	1000	270	15	68	8.7	52 ± 1	80	3	8.7	54 ± 1
		6	1000	270	35	22	8.7	43 ± 1	80	3	8.7	43 ± 1
	10/2018	9	1000	270	15	68	8.7	43 ± 1	80	3	8.7	44 ± 1
		16	1000	270	35	22	8.7	32 ± 1	80	3	8.7	32 ± 1
Regeneration temperature	8/2018	10	1000	270	25	38	8.7	18 ± 1	40	17	8.7	17 ± 1
		13	1000	270	25	38	8.7	33 ± 1	60	7	8.7	33 ± 1
Loading & regeneration RH	9/2017	4	1000	270	25	28	6.4	46 ± 1	80	2	6.4	46 ± 1
	10/2018	5	1000	270	25	0	0	36 ± 1	80	0	0	36 ± 1
		5	1000	270	25	30	6.9	39 ± 1	80	2	6.9	40 ± 1
Residence time	12/2017	1	1000	25	30	0	0	41 ± 2	65	4	7.4	not measured
		1	1000	50	30	0	0	40 ± 2	65	4	7.4	not measured
		1	1000	100	30	0	0	47 ± 1	65	4	7.4	not measured
		1	1000	250	30	0	0	49 ± 1	65	4	7.4	not measured

Figure 3 illustrates the CO_2 loading and regeneration capacity determined under reference conditions at different times over more than a year. Tests performed over a large number of cycles in September and October 2017 showed a stable capacity between 43 and 45 mg CO_2 per g sorbent for both adsorption and desorption. Subsequent measurements in April, August and October 2018 showed a moderate decline of the performance, with a final capacity between 39 and 40 mg CO_2 per g sorbent.

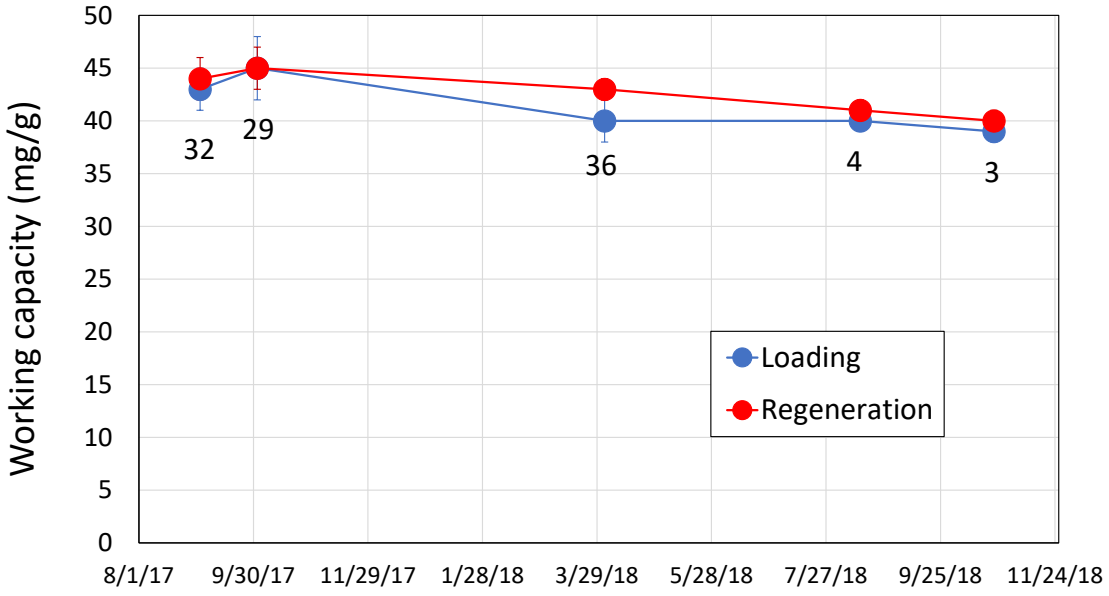

Figure 3. CO_2 working capacity determined during loading and regeneration under reference test conditions. The figures shown next to the results correspond to the number of L/R cycles used in each case to determine the working capacity.

The moderate loss of capacity is likely due to aging of the material over more than a year, even when there was no air circulation through the sorbent. The loss of performance was correlated with the exposure time, but not with the number of cycles, as the initial >60 cycles (9-10/2017) showed no significant degradation. By contrast, the major decrease of working capacity was

observed between 10/2017 and 11/2018, during which only 43 cycles were performed, rather than during the first 61 cycles. Overall, the capacity determined during regeneration was slightly higher than that determined during loading, although both determinations were within the experimental error. The gap is probably due to a systematic difference in the integration of the CO_2 breakthrough curves.

3.2 Influence of higher CO_2 concentration on sorbent performance

By increasing the challenge CO_2 concentration to 1600 ppm from 1000 ppm, the adsorption rate increased. The 900 ppm breakthrough endpoint was reached earlier: in 60 min at 1600 ppm vs. 290 min at 1000 ppm. The shorter adsorption period associated with a higher CO_2 challenge level resulted in a lower working capacity under this condition of 30 mg g^{-1} for adsorption and 34 mg g^{-1} for regeneration. The CO_2 concentration during regeneration was maintained at 400 ppm, and the endpoint at 410 ppm.

3.3 Influence of temperature and humidity on sorbent performance

CO_2 adsorption was affected by the loading and regeneration temperature and RH, as illustrated in Figure 4. Tests were carried out with loading temperatures of 15 and 35 °C in July 2017, and repeated in October 2018. The second test included also a test at 25 °C (reference conditions). The regeneration temperature (80 °C), loading RH (38%) and regeneration RH (3%) were maintained at the reference values in all cases. The observed decrease of the CO_2 adsorption capacity was proportional with increasing loading temperature, as shown in Figure 4A. The working capacity measured with a loading temperature of 35 °C was 17-25% lower than that at 15 °C, suggesting that operating the system at a low temperature can maximize the sorbent capacity. Figure 4A also shows a clear effect of sorbent aging in reducing the working capacity.

Additional tests were conducted by lowering the regeneration temperature from the reference condition (80 °C) to 60 °C and 40 °C. In these tests, the loading temperature (25 °C), loading RH (38%) and regeneration RH (3%) were maintained at reference levels. With the higher regeneration temperature, the working capacity was highest as a result of a more complete recovery of the sorbent (Figure 4B). However, the ratio between the relative change of adsorption capacity and temperature was the same for loading and regeneration temperature: 0.55 mg CO_2 per g sorbent per degree Celsius (Figure 4A and 4B).

Tests evaluating the effect of moisture content (absolute humidity) explored values between ~0 and 9 g m^{-3}, while keeping both loading (25 °C) and regeneration (80 °C) temperatures at their reference values. Changes in loading and regeneration RH had a moderate influence on the adsorption capacity (Figure 4C).

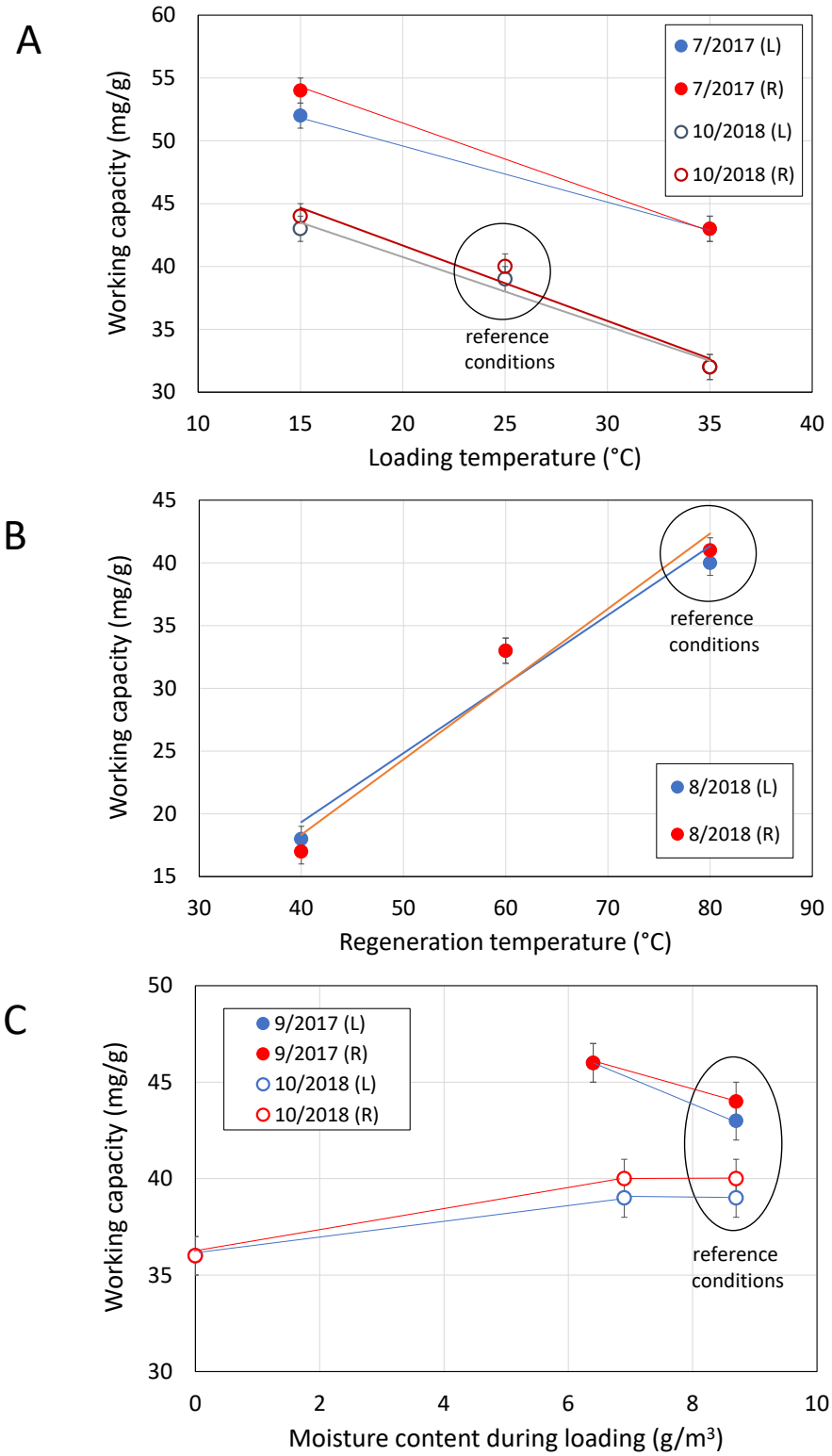

Figure 4. CO_2 adsorption capacity determined as a function of (A) loading temperature, (B) regeneration temperature and (C) moisture content (absolute humidity) during loading.

3.4 Influence of residence time on sorbent performance

The breakthrough curves corresponding to loading of the sorbent at four different face velocities (or residence times, R_t) are presented in Figure 5. Longer breakthrough times were observed as the residence time increased, with the two curves corresponding to the lowest values (R_t = 25 and 50 ms) showing initial downstream concentrations higher than 0 ppm (approximately 400 and 100 ppm, respectively). The reason for this incomplete CO_2 retention at higher face velocities is likely mass transfer limitations. The time required to reach quasi steady-state breakthrough conditions was approximately 20-30 min for experiments carried out at R_t = 25 and 50 ms. The same target was reached at nearly 50 min for R_t = 100 ms, and 120 min for R_t = 250 ms. The CO_2 working capacity increased with higher R_t in the range 40 – 49 mg CO_2 per g sorbent, as reported in Table 1. These changes illustrate the fact that, under the experimental non-equilibrium conditions, the adsorption process is not determined exclusively by the total number of active sites, but by those accessible to the air circulating through the sorbent.

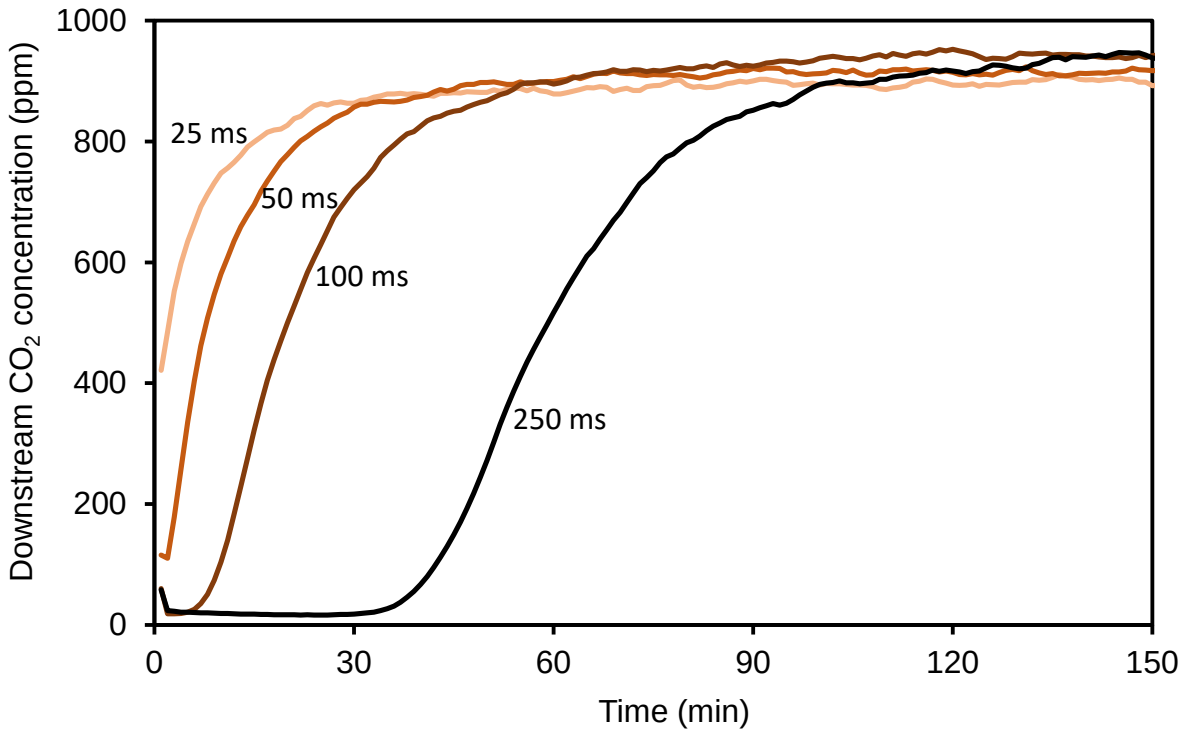

Figure 5. Breakthrough curves determined at four different residence times: 25, 50, 100 and 250 milliseconds. The working capacities determined in each case are reported in Table 1.

3.5 Describing CO_2 adsorption using simple partitioning models

The three kinetic models described in Table 2 had previously been used to fit CO_2 adsorption isothermal breakthrough curves, and were adapted from Shafeeyan et al (2015) [24]. The pseudo-first order model assumes reversible partition of CO_2 between gas and solid phases, the pseudo-second order model assumes chemical control of the adsorption kinetics, and the Avrami model is a variant of the pseudo-first order equation, incorporating an empirical exponent *n*. In these models, *t* is the time (min) elapsed from the beginning of the adsorption process, q_t is the amount of CO_2 (mg) adsorbed within a specific period *t*, and q_e represents the equilibrium capacity expressed in mg CO_2, corresponding to the maximum CO_2 adsorbed at a given temperature and face velocity (residence time). The corresponding kinetic constants for each model are k_F (first order), k_S (second order) and k_A (Avrami). The Avrami model also incorporates an empirical exponential parameter (*n*).

Table 2. Three adsorption models evaluated in this study, and parameters calculated for the reference test conditions during initial (9/2017) and final (10/2018) operation.

Model	Equation	Parameters (units)	Reference test conditions	
			9/2017	10/2018
Pseudo first order	$q_t = q_e(1 - e^{-k_F t})$	k_F (s^{-1})	9.8×10^{-5}	1.2×10^{-4}
		q_e (mol kg^{-1})	1.5	1.3
		Δq (%)	3.8	8.8
Pseudo second order	$q_t = \frac{q_e^2 k_s t}{1 + q_e k_s t}$	k_S (mol kg^{-1} s^{-1})	1.9×10^{-5}	3.5×10^{-5}
		q_e (mol kg^{-1})	2.7	2.1
		Δq (%)	3.4	9.3
Avrami	$q_t = q_e\left(1 - e^{-(k_A t)^n}\right)$	k_A (s^{-1})	1.1×10^{-4}	1.8×10^{-4}
		n	1.05	1.18
		q_e (mol kg^{-1})	1.4	0.98
		Δq (%)	2.0	4.0

.

Fitting was evaluated by considering the deviation between experimental results and values predicted by the kinetic models, applying the error function Δq, defined as [43]:

$$\Delta q(\%) = \sqrt{\frac{\sum\left[\left(q_{t(exp)} - q_{t(mod)}\right)/q_{t(exp)}\right]^2}{N-1}} \times 100 \qquad (9)$$

where $q_{t(exp)}$ is the amount adsorbed at a given time determined experimentally, $q_{t(mod)}$ is the amount adsorbed as predicted by the model, and N is the total number of experimental data points. The calculated error did not exceed 10% for any of the three types of kinetic models, as illustrated in Table 2 for experiments carried out under reference test conditions during initial (9/2017) and final cycles (10/2018). The Avrami model showed relatively lower Δq, but introduced an additional parameter. Considering that all models provided an acceptable fit, the pseudo-first-order model was used to model CO_2 adsorption. This model was successfully used to describe the adsorption kinetics of CO_2 on physical adsorbents such as activated carbon [18] and MCM- 41 molecular sieves [44]. The pseudo-first order kinetic model allows for a simple integration in algorithms to design, optimize and evaluate the performance of air cleaning systems. It can also be used to determine kinetic properties when the geometry of the particles is known [45]. This model assumes reversible interactions between the gas and solid surfaces [46], and is widely used in the description of fixed bed and cyclic CO_2 adsorption processes.

It should be noted that the equilibrium capacity q_e determined with the pseudo-first order model was 1.5 and 1.3 mol kg^{-1} for initial and final reference tests, respectively. These correspond to ~66 and 57 mg/g, which are higher than the reported working capacities in those tests. The main reason for this difference is that the working capacity was determined by interrupting loading when downstream CO_2 concentration reached 900 ppm, at a point in which the sorbent was far from saturation.

Both the equilibrium capacity and the adsorption rate constant were affected by changes in experimental parameters. In Figure 6, the predicted equilibrium capacity q_e is shown to correlate inversely with adsorption temperature, due to the exothermic nature of the adsorption process. By contrast, the kinetic rate constant (k_F) increased with temperature, consistent with increases in the rate of diffusion of CO_2 molecules inside the pores of sorbent, and higher chemical reaction rates. From the data shown in Figure 6, it can be observed that the relative reduction of the equilibrium capacity, of 18-23%, was larger than the relative increase in the adsorption rate, of 12-17%. Hence, the overall dependence on loading temperature shown in Figure 4A is dominated by changes in the equilibrium capacity. Results in Figure 6 show changes of the parameters over time that are consistent with the changes in the working capacity illustrated in Figure 3 for experiments carried out under reference tests conditions.

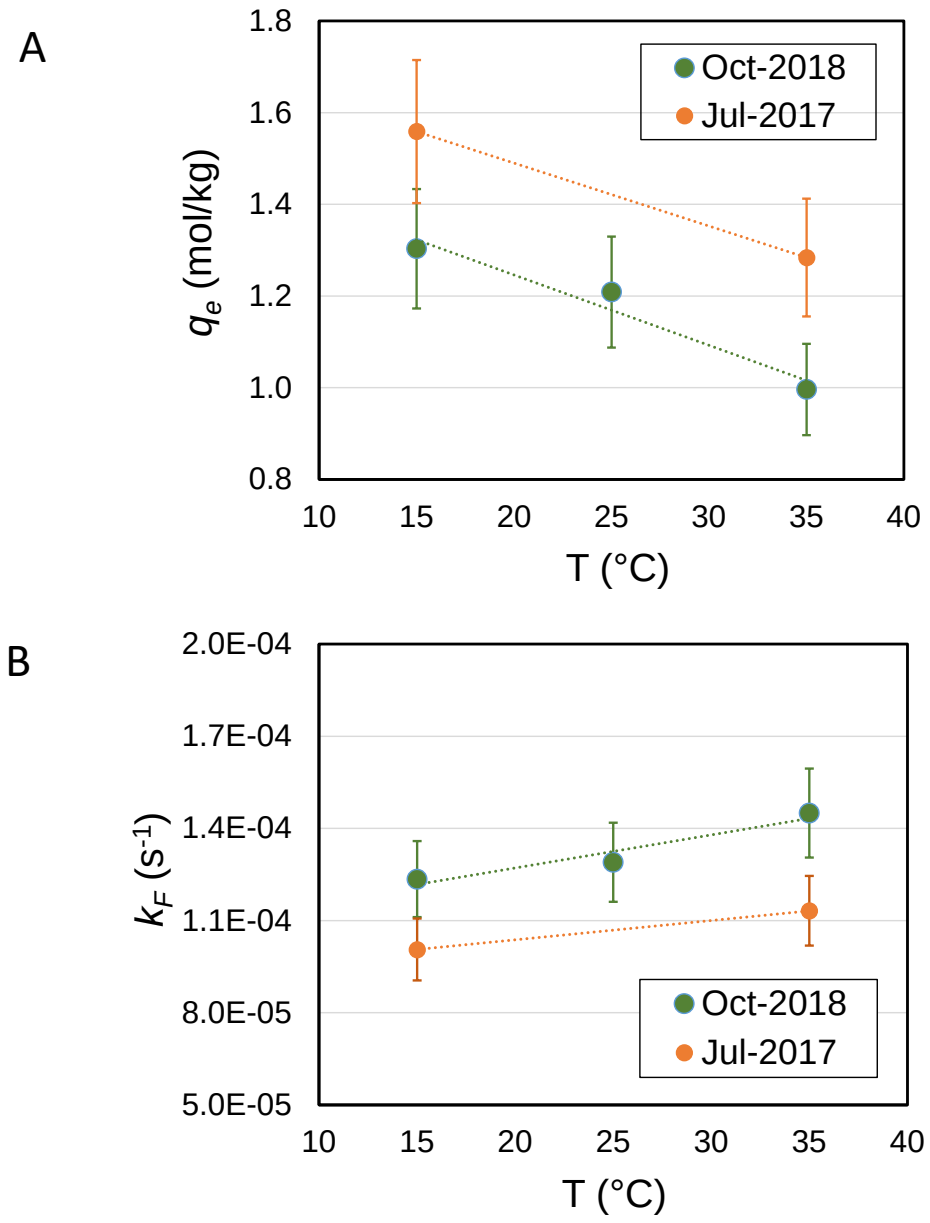

Figure 6. (A) Equilibrium capacities (q_e, mol kg^{-1}), and (B) kinetic rate constants (k_F, s^{-1}) determined at different loading temperatures with the pseudo first-order kinetic model. Error bars show ±10% of the calculated values.

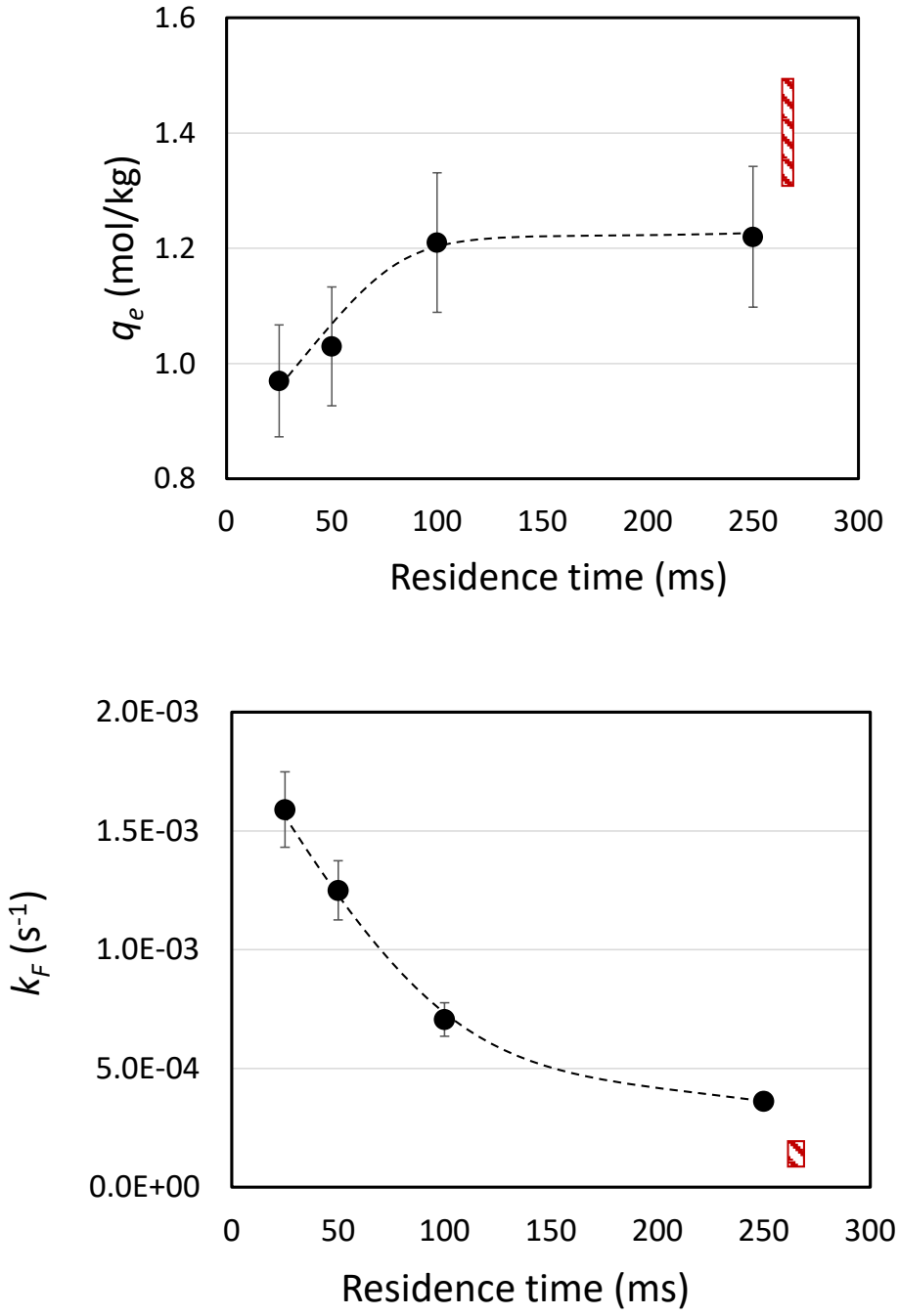

Figure 7. (A) Equilibrium capacities (q_e, mol kg^{-1}), and (B) kinetic rate constants (k_F, s^{-1}) determined at different residence times with the pseudo first-order kinetic model. Error bars show 10% standard deviation of the calculated value. The red striped bars correspond to values determined in reference test conditions at R_t = 270 ms, reported in Table 2.

The results presented in Figure 7 illustrate the changes in the first-order model parameters with increasing residence time. The equilibrium capacity grew with increasing *Rt,* reaching a plateau at the higher residence times. This result suggests that equilibrium capacity is a function of the face velocity, as the higher velocities tested here likely changed the adsorption equilibrium conditions at the boundary layer. By contrast, the rate constant decreased as the residence time increased. The equilibrium capacity q_e = 1.3 – 1.5 mol kg^{-1} determined for the automated system operating in reference conditions at *Rt* = 270 ms were higher than those determined for the highest residence time of 250 ms on the manual system, likely due to the fact that those experiments were carried out at different temperature and humidity. In particular, tests evaluating the effect of residence time were carried out using dry air, limiting the adsorption process to the reaction described in equation (1), not capturing additional CO_2 as bicarbonate in the presence of water, as described in equation (2).

3.6 Formaldehyde adsorption and desorption

The formaldehyde adsorption capacity was evaluated with integrated samples collected upstream and downstream, simultaneously, during the loading phase. Although formaldehyde was introduced continuously during all tests, sampling was carried out only in a sub-set of L/R cycles. The efficiency to adsorb and desorb formaldehyde was measured while the system was operating in reference conditions during two L/R cycles in September 2017 and six L/R cycles in April 2018. Formaldehyde was very effectively removed from the air stream, especially considering that the loading concentration (1.5 ± 0.6 ppb) was one to two orders of magnitude higher than typical indoor levels. During the loading period, a formaldehyde adsorption efficiency f_{ad} = 80-99% was calculated (Figure 8), corresponding to a capture capacity of 86 ± 36 µg g^{-1} sorbent. Variation of the capacity determined in different loading cycles correlated linearly to the varying challenge formaldehyde concentration. This was confirmed by performing linear regression between the two parameters resulting in R^2 >0.9 and intercept equal to 0 (Figure S3, Supporting Information), suggesting that the maximum adsorption capacity was not reached.

Unlike CO_2, formaldehyde was not desorbed completely from the sorbent during regeneration at 80 °C. A desorption efficiency of f_{de} = 10-69% was observed, as shown in Figure 8. This suggests that the reaction between the amine-impregnated material and formaldehyde was partially irreversible, and/or that the material has a large capacity to store formaldehyde, in

agreement with previous reports of formaldehyde adsorption to similar amine-based silica sorbents [34-36]. In the two series of formaldehyde data, the first L/R cycle shows significantly lower desorption efficiency (f_{de} = 10-16 %) than several cycles of the same series (f_{de} = 48-69 %). One possible explanation for such initial lower desorption is the presence of a higher moisture content in the sorbent due to equilibration with ambient air during idle periods, as compared with dryer conditions achieved immediately after regeneration.

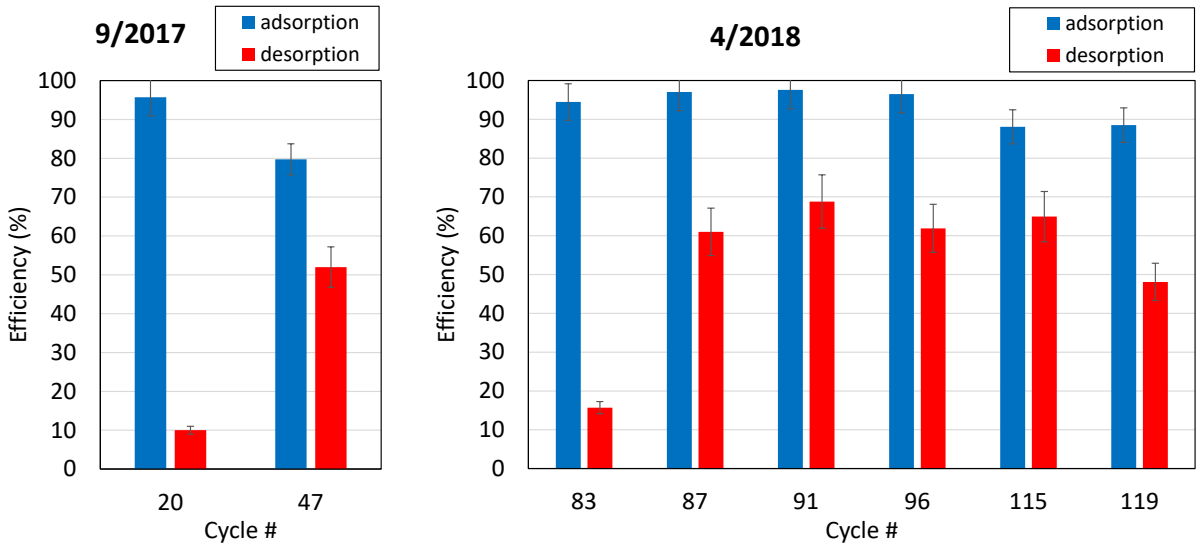

Figure 8. Formaldehyde adsorption efficiency (f_{ad}) and desorption efficiency (f_{de}) determined in different cycles during tests performed in reference conditions in September 2017 (32 cycles) and April 2018 (36 cycles). The cycle number corresponds to the overall set of experiments, from which #20 and #83 were the first cycles of each of the two tests presented here.

4 Implications

The pseudo-first order kinetic model described the adsorption kinetics of CO_2 throughout the range of temperature tested in this study, suggesting that the adsorption process is primarily due to reversible chemisorption. This simple model can be used to predict the behavior of a sorbent bed treating recirculated building air. The measured CO_2 capacity at different temperatures

commonly found in buildings suggest that keeping the sorbent bed at relatively low temperatures has a positive effect in the loading capacity of the sorbent. Instead, operating the sorbent at the relatively high temperatures commonly found in a non-air conditioned machine room during the summer can lead to reduced performance. This temperature effect is in line with the observed trends for equilibrium and kinetic parameters as a function of temperature.

The working capacity determined in this study can be used to predict the amount of sorbent required to maintain CO_2 levels below a certain target concentration in commercial buildings. ASHRAE Standard 62.1 requires a minimum of 5 cfm per person to address occupant-associated indoor contaminants, which include but are not limited to CO_2. The IAQ procedure allows for reduction of outdoor air using engineered air cleaning systems [8]. The sorbent studied here could be part of the solution for occupant-associated contaminants. Considering that the average amount of CO_2 emitted by a resting adult is 34 g h^{-1} [22], the mass of sorbent required to prevent CO_2 concentration to increase beyond 1000 ppm is approximately 2 kg per person. This estimation assumes that the sorbent is placed in the return loop to defer an equivalent amount of outdoor air over four hours of daily operation in loading mode, with nighttime regeneration, as a peak reduction strategy. The predicted sorbent mass is comparable to amounts of granular activated carbon (GAC) recommended for HVAC systems operating in conditions of severe outdoor air pollution [47].

While the main motivation for operating air cleaners containing this sorbent is reducing indoor CO_2 concentrations, these materials show great potential also for scrubbing formaldehyde from indoor air. Unlike CO_2, formaldehyde accumulates over time in the sorbent. However, during the almost 200 loading/regeneration cycles reported here, there was no saturation of formaldehyde despite being challenged with concentrations that were one to two orders of magnitude higher than those commonly found in buildings. For future application in real-world scenarios, the reversibility of formaldehyde chemisorption on amine-modified sorbents should be explored in more detail, to assess the possibility of materials saturated with formaldehyde becoming a potential pollutant source. Previous studies on similar aminosilicas suggested that release of adsorbed formaldehyde at room temperature is unlikely. Nomura and Jones showed that adsorbed aldehydes (including formaldehyde) are stably attached to amines on the silica surface, with no loss observed after one week of storage under an ambient atmosphere [35]. The same authors reported adsorbed formaldehyde on two types of porous aminosilicas did not desorb at

temperatures below 130 °C [36]. Ewlad-Ahmed et al observed permanent removal of formaldehyde from indoor air under dynamic chamber conditions comparable to our experiments [34]. These observations coincide with the low desorption efficiency determined in our study. Similarly, the presence of formaldehyde did not affect dramatically the sorbent's ability to capture CO_2, nor its regeneration efficiency.

Acknowledgement

This research was supported by the US-China Clean Energy Research Center – Building Energy Efficiency (CERC-BEE) Program and the Assistant Secretary for Energy Efficiency and Renewable Energy, U.S. Department of Energy under Contract No. DEAC02-05CH11231. The authors thank Spencer Dutton (LBNL) and William Delp (LBNL) for their contributions to this study.

References

[1] T.A. Boden, G. Marland, R.J. Andres, Global, regional, and national fossil-fuel CO_2 emissions, (2011). https://cdiac.ess-dive.lbl.gov/trends/emis/overview.html

[2] U.S. Energy Information Administration, Emissions of greenhouse gases in the US, (2015). https://www.eia.gov/environment/emissions/ghg_report/ghg_overview.php

[3] W. Fisk, D. Black, G. Brunner, Changing ventilation rates in U.S. offices: Implications for health, work performance, energy, and associated economics, Building and Environment (2012) 47, 368-372.

[4] X. Zhang, P. Wargocki, Z. Lian, C. Thyregod, Effects of exposure to carbon dioxide and bioeffluents on perceived air quality, self-assessed acute health symptoms, and cognitive performance, Indoor Air 27 (2017) 47-64.

[5] M.G. Apte, W.J. Fisk, J.M. Daisey, Associations between indoor CO2 concentrations and sick building syndrome symptoms in US office buildings: AN analysis of the 1994-1996 BASE

study data, Indoor Air 10 (2000) 246-257. https://doi.org/10.1034/j.1600-0668.2000.010004246.x

[6] P. Wargocki, D.P. Wyon, J. Sundell, G. Clausen, P.O. Fanger, The effects of outdoor air supply rate in an office on perceived air quality, sick building syndrome (SBS) symptoms and productivity, Indoor Air 10 (2000) 222-236. https://doi.org/10.1034/j.1600-0668.2000.010004222.x

[7] A. Persily, Challenges in developing ventilation and indoor air quality standards: The story of ASHRAE Standard 62, Building and Environment 91 (2015) 61-69.

[8] ANSI/ASHRAE Standard 62.1-2019, Ventilation for Acceptable Indoor Air Quality, https://ashrae.iwrapper.com/ViewOnline/Standard_62.1-2019 (2019).

[9] O.A. Seppänen, W.J. Fisk, M.J. Mendell, Association of ventilation rates and CO_2 concentrations with health and other responses in commercial and institutional buildings, Indoor Air 9 (1999) 226-252. 10.1111/j.1600-0668.1999.00003.x

[10] U. Satish, M.J. Mendell, K. Shekhar, T. Hotchi, D. Sullivan, S. Streufert, W.J. Fisk, Is CO2 an indoor pollutant? direct effects of low-to-moderate CO2 concentrations on human decision-making performance, Environ Health Persp 120 (2012) 1671-1677.

[11] R. Maddalena, M.J. Mendell, K. Eliseeva, W.R. Chan, D.P. Sullivan, M. Russell, U. Satish, W.J. Fisk, Effects of ventilation rate per person and per floor area on perceived air quality, sick building syndrome symptoms, and decision-making, Indoor Air 25 (2015) 362-370.

[12] J.G. Allen, P. MacNaughton, U. Satish, S. Santanam, J. Vallarino, J.D. Spengler, Associations of cognitive function scores with carbon dioxide, ventilation, and volatile organic compound exposures in office workers: A controlled exposure study of green and conventional office environments, Environ Health Persp 124 (2016) 805-812.

[13] J.G. Allen, P. MacNaughton, J.G. Cedeno-Laurent, X. Cao, S. Flanigan, J. Vallarino, F. Rueda, D. Donnelly-McLay, J.D. Spengler, Airplane pilot flight performance on 21 maneuvers in a flight simulator under varying carbon dioxide concentrations, J. Exposure Sci. Environ. Epidemiol. 29(4) (2019) 457-468. doi: 10.1038/s41370-018-0055-8

[14] W.J. Fisk, P. Wargocki, X. Zhang, Do indoor CO2 levels directly affect perceived air quality, health, or work performance?, ASHRAE Journal 61(9) (2019) 70-77.

[15] Y. Belmabkhout, R. Serna-Guerrero, A. Sayari, Amine-bearing mesoporous silica for CO2 removal from dry and humid air, Chemical Engineering Science 65 (2010) 3695-3698. 10.1016/j.ces.2010.02.044

[16] R. Serna-Guerrero, E. Da'na, A. Sayari, New insights into the interactions of CO2 with amine-functionalized silica, Industrial & Engineering Chemistry Research 47 (2008) 9406-9412. 10.1021/ie801186g

[17] S.C. Lee, C.C. Hsieh, C.H. Chen, Y.S. Chen, CO2 adsorption by Y-type zeolite impregnated with amines in indoor air, Aerosol and Air Quality Research 13 (2013) 360-366. doi: 10.4209/aaqr.2012.05.0134

[18] Z. Zhang, W. Zhang, X. Chen, Q. Xia, Z. Li, Adsorption of CO2 on zeolite 13X and activated carbon with higher surface area, Separation Science and Technology 45 (2010) 710-719. 10.1080/01496390903571192

[19] P.J.E. Harlick, A. Sayari, Applications of pore-expanded mesoporous silicas. 3. Triamine silane grafting for enhanced CO2 adsorption, Industrial & Engineering Chemistry Research 45 (2006) 3248-3255. 10.1021/ie051286p

[20] S. Loganathan, M. Tikmani, S. Edubilli, A. Mishra, A.K. Ghoshal, CO2 adsorption kinetics on mesoporous silica under wide range of pressure and temperature, Chemical Engineering Journal 256 (2014) 1-8. https://doi.org/10.1016/j.cej.2014.06.091

[21] A. Nomura, C.W. Jones, Airborne aldehyde abatement by latex coatings containing amine-functionalized porous silicas, Ind. Eng. Chem. Res. 54 (2015) 263-271. doi: 10.1021/ie504165d

[22] P.E. Rajan, A. Krishnamurthy, G. Morrison, F. Rezaei, Advanced buffer materials for indoor air CO2 control in commercial buildings, Indoor Air 27 (2017) 1213-1223. doi: 10.1111/ina.12386

[23] D.P. Bernabe, R.A.S. Herrera, B.T. Doma, M.-L. Fu, Y. Dong, Y.F. Wang, Adsorption of low concentration formaldehyde in air using ethylene-diamine-modified diatomaceous earth, Aerosol and Air Quality Research 15 (2015) 1652-1661. doi: 10.4209/aaqr.2015.05.0292

[24] M.S. Shafeeyan, W.M.A.W. Daud, A. Shamiri, N. Aghamohammadi, Modeling of carbon dioxide adsorption onto ammonia-modified activated carbon: Kinetic analysis and breakthrough behavior, Energy & Fuels 29 (2015) 6565-6577. 10.1021/acs.energyfuels.5b00653

[25] E.F. da Silva, H.F. Svendsen, Computational chemistry study of reactions, equilibrium and kinetics of chemical CO2 absorption, International Journal of Greenhouse Gas Control 1 (2007) 151-157. https://doi.org/10.1016/S1750-5836(07)00022-9

[26] B. Arstad, R. Blom, O. Swang, CO2 absorption in aqueous solutions of alkanolamines: mechanistic insight from quantum chemical calculations, The Journal of Physical Chemistry A 111 (2007) 1222-1228. 10.1021/jp065301v

[27] S. Choi, J.H. Drese, C.W. Jones, Adsorbent materials for carbon dioxide capture from large anthropogenic point sources, ChemSusChem 2 (2009) 796-854. doi:10.1002/cssc.200900036

[28] A. Sayari, Y. Belmabkhout, Stabilization of amine-containing CO2 adsorbents: dramatic effect of water vapor, Journal of the American Chemical Society 132 (2010) 6312-6314. 10.1021/ja1013773

[29] X. Xu, C. Song, B.G. Miller, A.W. Scaroni, Adsorption separation of carbon dioxide from flue gas of natural gas-fired boiler by a novel nanoporous “molecular basket” adsorbent, Fuel Processing Technology 86 (2005) 1457-1472. https://doi.org/10.1016/j.fuproc.2005.01.002

[30] T. Salthammer, Formaldehyde sources, formaldehyde concentrations and air exchange rates in European housings, Building and Environment 150 (2019) 219-232.

[31] T. Salthammer, S. Mentese, R. Marutzky, Fromaldehyde in the indoor environment, Chem. Rev. 110 (2010) 2536-2572.

[32] H. Chen, J. Mo, R. Xiao, E. Tian, Gaseous formaldehyde removal: A laminated plate fabricated with activated carbon, polyimide, and copper foil with adjustable surface temperature and capable of in situ thermal regeneration, Indoor Air 29 (2019) 469-476. DOI: 10.1111/ina.12540

[33] R. Xiao, J. Mo, Y. Zhang, D. Gao, An in-situ thermally regenerated air purifier for indoor formaldehyde removal, Indoor Air 28 (2018) 266-275. DOI: 10.1111/ina.12441

[34] A.M. Ewlad-Ahmed, M.A. Morris, S.V. Patwardhan, L.T. Gibson, Removal of formaldehyde from air using functionalized silica supports, Environmental Science & Technology 46 (2012) 13354-13360. 10.1021/es303886q

[35] A. Nomura, C.W. Jones, Amine-functionalized porous silicas as adsorbents for aldehyde abatement, ACS Applied Materials & Interfaces 5(12) (2013) 5569-5577. 10.1021/am400810s

[36] A. Nomura, C.W. Jones, Enhanced formaldehyde-vapor adsorption capacity of polymeric amine-incorporated aminosilicas, Chem. Eur. J. 20 (2014) 6381-6390. 10.1002/chem.201304954

[37] M.L. Campbell, F.D. Guerra, J. Dhulekar, F. Alexis, D.C. Whitehead, Target-specific capture of environmentally relevant gaseous aldehydes and carboxylic acids with functional nanoparticles, Chem. Eur. J. 21 (2015) 14834-14842. 10.1002/chem.201502021

[38] E.R. Monazam, J. Spenik, L.J. Shadle, Fluid bed adsorption of carbon dioxide on immobilized polyethylenimine (PEI): Kinetic analysis and breakthrough behavior, Chemical Engineering Journal 223 (2013) 795-805. https://doi.org/10.1016/j.cej.2013.02.041

[39] R. Kimura, M. Buelow, J. Kauffman, P. Tran, S. Shum, J. Levine, W. Ruettinger, D. Weinberger, Carbon dioxide sorbents for air quality control, Patent application WO2017139555 https://patentscope.wipo.int/search/en/detail.jsf?docId=WO2017139555 (2017).

[40] S.J. Reynolds, D.W. Black, S.S. Borin, G. Breuer, L.F. Burmeister, L.J. Fuortes, T.F. Smith, M.A. Stein, P. Subramanian, P.S. Thorne, P. Whitten, Indoor environmental quality in six commercial office buildings in the midwest United States, Applied Occupational and Environmental Hygiene 16 (2001) 1065-1077. 10.1080/104732201753214170

[41] X. Wu, M.G. Apte, R. Maddalena, D.H. Bennett, Volatile organic compounds in small- and medium-sized commercial buildings in California, Environmental Science & Technology 45 (2011) 9075-9083. 10.1021/es202132u

[42] USEPA, Compendium method TO-11A - Determination of formaldehyde in ambient air using adsorbent cartridge followed by HPLC [Active Sampling Methodology], (1999).

[43] A.M.M. Vargas, A.L. Cazetta, M.H. Kunita, T.L. Silva, V.C. Almeida, Adsorption of methylene blue on activated carbon produced from flamboyant pods (Delonix regia): Study of adsorption isotherms and kinetic models, Chemical Engineering Journal 168 (2011) 722-730. 10.1016/j.cej.2011.01.067

[44] Á. Berenguer-Murcia, A.J. Fletcher, J. García-Martínez, D. Cazorla-Amorós, Á. Linares-Solano, K.M. Thomas, Probe molecule kinetic studies of adsorption on MCM-41, The Journal of Physical Chemistry B 107 (2003) 1012-1020. 10.1021/jp026764d

[45] R.M.A. Roque-Malherbe, Adsorption and diffusion in nanoporous materials, CRC Press, Boca Raton, FL, 2018.

[46] J. Yang, C.-H. Lee, Adsorption dynamics of a layered bed PSA for H2 recovery from coke oven gas, AIChE Journal 44 (1998) 1325-1334. doi:10.1002/aic.690440610

[47] ASHRAE Handbook 2019 - HVAC Applications. American Society of Heating, Refrigerating and Air-Conditioning Engineers, Atlanta GA (2019) https://www.ashrae.org/technical-resources/ashrae-handbook.

SUPPORTING INFORMATION

Performance of a CO_2 sorbent for indoor air cleaning applications: Effects of environmental conditions, sorbent aging, and adsorption of co-occurring formaldehyde

Xiaochen Tang[1], Sébastien Houzé de l'Aulnoit[1], Mark T. Buelow[2], Jonathan Slack[1], Brett C. Singer[1], Hugo Destaillats[1,*]

1. Indoor Environment Group, Lawrence Berkeley National Laboratory, Berkeley CA, USA.

2. BASF Corporation, Iselin NJ, USA.

* Corresponding Author E-mail: HDestaillats@lbl.gov

Table S1: Evaluation of different loading endpoint values at 50% and 9% relative humidity

Endpoint	**CO_2 capacity at RH~50% (mg CO_2 per g sorbent)**	**Fraction of consumed capacity**	**CO_2 capacity at RH~9% (mg CO_2 per g sorbent)**	**Fraction of consumed capacity**	**Difference (%)**
700ppm	37.7	85%	42.4	86%	11%
800ppm	40.8	92%	45.7	93%	11%
900ppm	44.3	100%	49.1	100%	9.8%

Figure S1: Example of (A) temperature measured at the outer surface of chamber and in the air flow downstream of the sorbent, and (B) relative humidity measured upstream and downstream of the sorbent, at room temperature (20 °C).

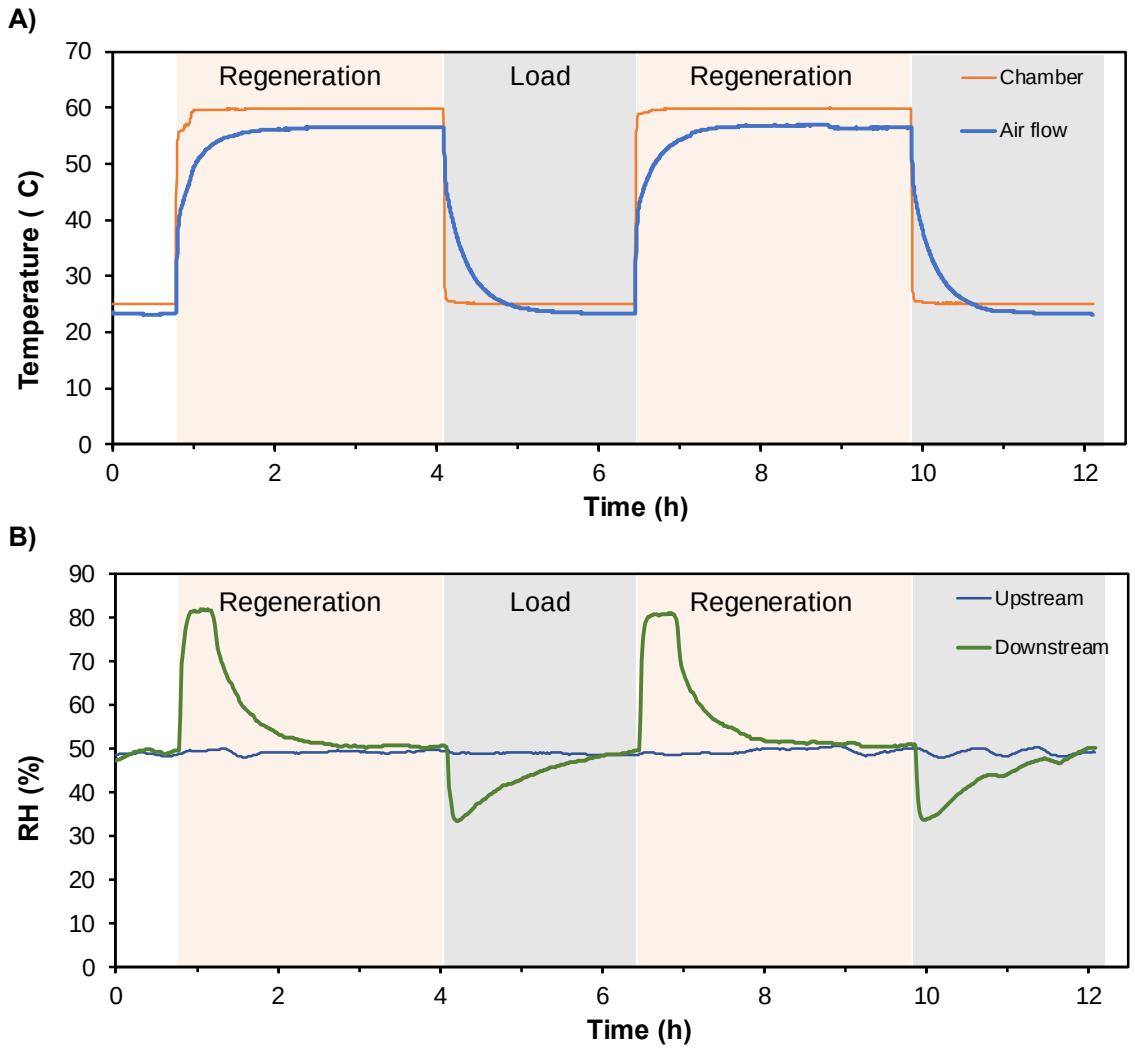

The sorbent temperature changed almost instantaneously upon switching between loading and regeneration phases, but the air temperature took longer (~60 min) to equilibrate (Figure S1). The temperature difference between the sorbent and air was within 2°C. Changes in moisture content (measured as RH at ambient temperature in Figure S1) followed the same patterns

observed for CO_2, as water vapor was also captured and released by the sorbent. In the loading phase, water in the air flow was retained by the sorbent, leading to a lower downstream RH, which slowly reached equilibrium with the upstream. When the sorbent was heated during the regeneration phase, water was quickly released back into the air.

Figure S2: Measurement of CO_2 sorption and desorption capacity in multiple cycles. (A) Breakthrough isotherms during 36 consecutive adsorption/desorption cycles; (B) CO_2 capacity determined in each of the cycles.

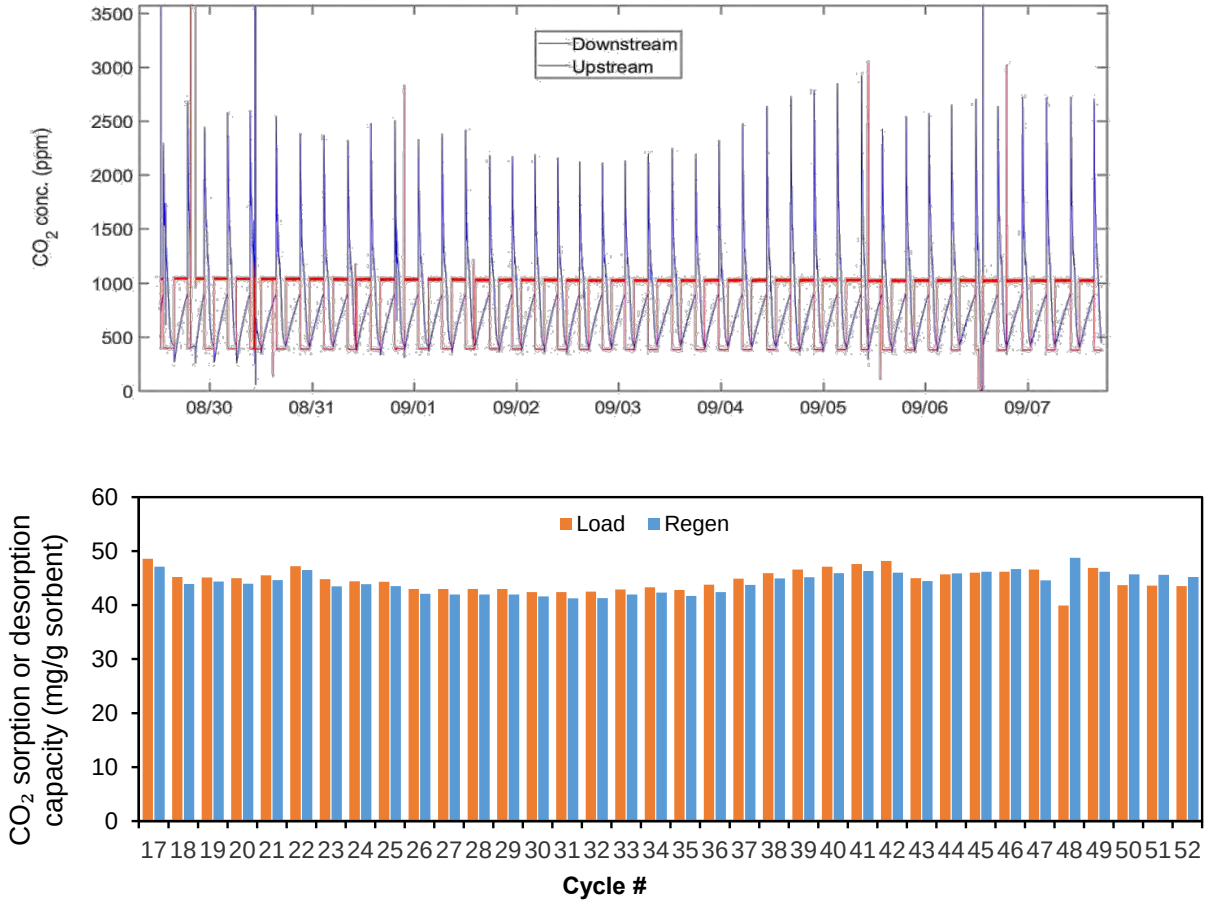

Figure S3: Linear correlation between formaldehyde adsorption capacity and challenge concentration.